2003－CVIM－140　(5)
2003／9／8

織布反射のレンダリング方法

楊　進華　　池内　克史

本研究では，織布を構成される繊維と糸の二つの要点に基づいて,物理的な反射モデルを提案する。布の材料特徴を考え，物理学の拡散方程によって，一般的繊維表面の反射モデルを作る。そして，繊維の様々な端面形状を考える上，繊維から糸をシミュレションする幾何モデルを提案し，糸の表面からの反射特性を推定する。布の織り方による様々な布の反射は，提案した糸の反射モデルでシミュレションすることが可能になる。本論文は，この手法の理論とともに，実物体による実験結果を示し，その有効性を示した。

A Rendering Method for Woven Clothes Reflections

Jinhua Yang　　Katsushi Ikeuchi

We proposed a physics-based rendering method for reflection of woven textiles. Both reflection properties of fibers and yarns are taken into account, which are the primary factors affecting visual appearance of cloths. The reflection from fiber surfaces is analyzed using Kirchhoff diffraction theory, assuming a statistical surface. Yarns are usually consisted of a group of fibers and they are simulated by a group of parallel infinite long triangle prisms which considers the different cross section shapes of fibers. The reflections from yarns are derived according to such geometry, taking into account of masking and shadowing. The model is compared with experimental data from spectrophotometer measurement on different woven textile samples and fit very well by numerical simulations. Theoretically the model is suitable to different kinds of woven textile structure and fiber materials. Also it can be developed to be used in computer graphics applications.

1. Introduction

Woven cloth simulation is an interesting and important issue for fashion design, human animation, interior design and other fields of CG and CV applications. There are mainly two different directions for the researches, one is focused on the investigation of physical and mechanical phenomena of woven clothes, such as deformation, wrinkling and crumpling, and the other is about the optical appearance of the cloth, including texturing and illumination effects. While it has been developed in the former area, the research on illumination models for cloth is much less advanced. It is difficult to build a simple physically based illumination model to simulate a cloth because of the different weaving structure of cloth and the complex microstructure of each thread.

The surface of woven clothes is usually regarded as one kind of rough surface and reflection is usually assumed to be Lambertian. In fact, such rendering is not accurate and not enough, and not all of clothes appears to be Lambertian in reflection. The properties of cloth materials and cloth structures should be taken into account.

Light incident on a surface may be absorbed, reflected and/or transmitted. The reflected light can be in a specific direction, in such case it is called specular reflection, and it can also be uniform with no specific direction, which is called diffuse reflection, both are related with light wavelength and material properties. For reflection from rough surfaces, it is a more complicated, statistical process including multi reflection, diffraction and interference effects related with the microstructure of the surface. Lambert model and Phong model have been proposed to describe the diffuse reflection and specular reflection from rough surface respectively and are still widely used in computer graphics and machine vision. However, there are many applications in which these two models can prove to be inaccurate[1].

The reflectance models of rough surface have been widely researched in the past decades and many achievements have been made. Torrance and Sparrow [2] proposed a BRDF reflectance model based on geometrical optics, describing specular reflection from rough surfaces. In their model, the surface is modeled as a collection of V-cavities with specular reflection and the distribution of surface normals is assumed to be normal. Cook and Torrance[3] improved Torrance and Sparrow model to implement shading in computer graphics. A diffuse term and an overall ambient term are added in their model. Poulin and Fourier[4] derived a reflection model for anisotropic surface. The anisotropy is simulated by small cylinders distributed on the surface. Different levels of anisotropy are achieved by varying the distance between each cylinder and/or rising the cylinders more or less from

東京大学大学院学際情報学府
Graduate School of Interdisciplinary Information Studies, the University of Tokyo

the surface. Multidirectional anisotropy is modeled by orienting groups of cylinders in different direction. The model takes into account masking and shadowing between cylinders while neglecting effects caused by intnerreflection. Oren and Nayar[1] presented an improved Lambertian model which can be applied to isotropic as well as anisotropic rough surface. The model is based on the same surface model as the Torrance-Sparrow model but assumes the facets to be Lambertian in reflection. It takes into account complex geometrical effects such as masking, shadowing and interreflections between points on the surface. He[5] suggested a general reflectance model based on physical optics and described specular refelction, directional diffuse and uniform diffuse reflection by a surface. The surface has statistical properties and its height is assumed to be Gaussian distributed and spatially isotropic.

The reflectance models above have assumed microscopic facets to be specular or Lambertian in reflection, and most of them are based on geometrical optics. The complex material properties of fibers have suggested that these assumptions above are not appropriate and it is better to be analyzed based on physical optics. Nayar etc.[6] studied reflectance models based on physical optics and geometrical optics in detail and proposed a general reflectance framework containing three components: specular reflection, directional diffuse reflection and uniform diffuse reflection. In practices, not all the three parts have the same effects in reflection process and some can be neglected to simplify calculation and rendering.

There are only a few researches specified in woven cloth simulations reported in the literature. Evelyn[7] presents a simple approach to simulate a woven cloth. Two cloth models are built by procedural method texturing method and bump mapping. The anisotropic reflection on the surfaces of the threads is created by approximating the BRDF by Schlick[8]. Volevich[9] considered the real 3D structure of the cloth at micro level and provided a lighting simulation method in BSDF form with ray tracing by virtual goniometric spectrophotometer(VGSP). Usami[10] provided an anisotropic reflectance model for cloth by reflectivity measurements and surface interpolation. The reflectivity of cloth in different directions was measured by high quality goniometric spectro-photometer and the anisotropic reflection characteristics were abstracted, then by NURBS surface modeling method the reflectance function was constructed.

We proposed a general modeling method for reflection of woven clothes, taking into account the materials properties and weaving structure properties. Most textiles are produced by twisting fibers into yarns and then knitting or weaving yarns into a fabric. Woven fabrics are made of two sets of yarns, a lengthwise set called the warp and a crosswise set called the weft. The elastic behavior of woven structure depends predominantly on the elastic properties of the yarns used to manufacture them. Woven fabrics are classified as to weave or structure according to the manner in which warp and weft cross each other. The three fundamental weaves are the plain, twill, and satin. Figure 1 shows the basic structure of

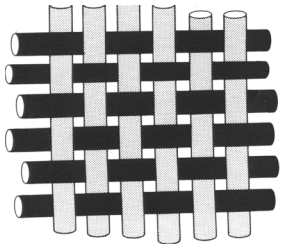

Figure 1: The basic structure of plain woven cloth

woven clothes. The reflection from cloth relies on that of yarns and the woven structures. Fibers are the raw materials for all fabrics. Some fibers occur in nature as fine strands that can be twisted into yarns. These natural fibers come from plants, animals, and minerals. For most of history, people had only nature fibers to use in making cloth. But modern science has learned how to produce fibers by chemical and technical means. The chief fibers manufactured from petrochemicals include nylon, polyester, acrylic, and olefin. Yarns are made from fibers so the reflection from fibers has great effects on reflection characteristics of yarns. The reflection from fiber surface are analyzed by Kirchhoff diffraction function, then that of yarn surface was analyzed according to the geometrical top structure, from regularly arrangements to random profile structures for different woven cloth structures.

2. Reflection from fibers surface

2.1 light scattering of material surfaces

Represent the electric field of an incident light wave by E_1 and the electric field of the scattered wave by E_2. When the source is far away from surface, the incident light can be regarded as a harmonic plane wave:

$$E_1 = E_{10} e^{i(\vec{k}_1 \cdot \vec{r} - \omega t)} \quad (1)$$

where $\vec{k}_1$ and E_{10} are the propagation vector and the amplitude of incident light respectively, $\vec{r}$ is the vector coordinate of the point in space at which the field is measured and ϖ the radian frequency. Let $\vec{P}$ be an observation point and let $\vec{R}$ be the vector from $\vec{P}$ to the point $\vec{r}$ on surface A. Then the intensity E_2 of the scattered field at $\vec{P}$ is given by the Helmholtz integral:

$$E_2(\vec{P}) = \frac{1}{4\pi}\iint_A \left(E_A(\vec{r})\frac{\partial \psi}{\partial n} - \psi \frac{\partial E_A(\vec{r})}{\partial n} \right) dA \quad (2)$$

where $\psi = \frac{e^{ik_2 R'}}{R'}$ is the free space Green's function and $E_A(\vec{r})$ is scattered filed at point $\vec{r}$ on the surface.

The solution to this equation as a function of reflection surface A is difficult under most circumstances because of the surface complexities. As have been done by others, we will consider a rough surface to have a statistical distribution. Since the surface is assumed to be a random process, it causes in turn the scattered electric field to be a random variable. The expected value of the field can then be solved under some probability distribution assumptions. What we are interested in is the expected value of the squared magnitude of the scattered electric field and can be written as:

$$\left\langle E_2 E_2^* \right\rangle = \left| E_{20} \right|^2 \cdot \Omega(\theta_i, \theta_r, \phi_i, \phi_r, \sigma_h, \tau) \quad (3)$$

where $\theta_i, \phi_i, \theta_r, \phi_r$ denote polar and azimuth angles of incident light and sensor direction respectively, σ_h and τ are parameters used to describe rough surface which are *rms* roughness of the surface and the autocorrelation length respectively. E_{20} is the electric field in the specular direction, $\theta_i = \theta_r$, by a smooth surface under the same angle of incident, hence, it satisfies $E_{20} = F(\theta_i, n)E_1$, where F is the Fresnel reflection. Ω is geometrical scattering function which describes the distribution of reflection. It should satisfy the following expression according to rule of energy conservations:

$$\iint \Omega(\theta_i, \phi_i, \theta_r, \phi_r, \sigma_h, \tau) d\theta_r d\phi_r \le 1 \quad (4)$$

Because some reflected light may be reradiated by multi-reflection due to rough surface, all energy in once surface reflection process calculated above may be smaller than 1.

2.2 Surface radiance

Human beings can not directly perceive the electric field. We see that an area of surface has a particular brightness. The perceived brightness is related to the electric field through a radiance equation.

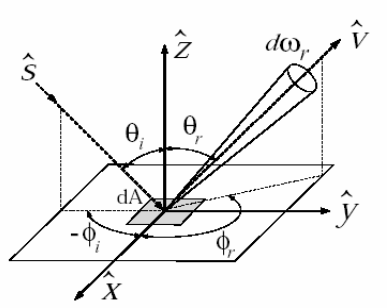

Figure 2: Geometry used to define radiaometric terms

Figure 2 shows the definition of radiance of a surface element dA illuminated from the direction $\hat{s} = (\theta_i, \phi_i)$ and viewed by a sensor in the direction $\hat{v} = (\theta_r, \phi_r)$. The radiance of a surface patch dA is the light flux emitted per unit foreshortened area per unit solid angle:

$$dL_r = \frac{d\Phi_r}{dA\cos\theta_r d\omega_r} \quad (5)$$

where $d\Phi_r$ is the flux radiated into an infinitesimal solid angle $d\omega_r$, $dA\cos\theta_r$ is the foreshortened area as viewed from θ_r.

The reflectance of a surface is usually represented by the *Bi-directional Reflectance Distribution Function* (*BRDF*). The *BRDF* is defined as the ratio of radiance to irradiance of the surface:

$$f_r(\theta_i, \phi_i, \theta_r, \phi_r) = \frac{dL_r(\theta_i, \phi_i, \theta_r, \phi_r)}{dE_i(\theta_i, \phi_i)} \quad (6)$$

where dL_r is the surface radiance which depends ont the direction of illumination and the sensor direction, and dE_i is the irradiance of the surface by the light incident from the direction (θ_i, ϕ_i).

The *BRDF* of the surface considered is

$$f_r = \frac{\left|F\right|^2 \cdot \Omega(\theta_i, \phi_i, \theta_r, \phi_r, \sigma_h, \tau)}{\cos\theta_i d\omega_r} \quad (7)$$

For the expression of geometrical scattering function Ω, we assume it has the following form:

$$\Omega = \beta \cdot G \cdot S \quad (8)$$

where β is normalization constant, G is geometrical scattering coefficient and S is Shadowing function. For G, we adopt He's scattering coefficient of a random rough surface[5]:

$$G = e^{-g}\left[\Delta + \frac{d\omega_i}{\pi\cos\theta_r} Q \cdot D \right] \quad (9)$$

where

$$Q = \left(\frac{\vec{v}\cdot\vec{v}}{v_z} \right)^4 \frac{1}{\left| \hat{k}_r \times \hat{k}_i \right|^4} \cdot \left[\left(\hat{s}_r \cdot \hat{k}_i \right)^2 + \left(\hat{p}_r \cdot \hat{k}_i \right)^2 \right] \left[\left(\hat{s}_i \cdot \hat{k}_r \right)^2 + \left(\hat{p}_i \cdot \hat{k}_r \right)^2 \right]$$

$$D = \frac{\pi^2 \tau^2}{4\lambda^2} \sum_{m=1}^{\infty} \frac{g^m}{m!m} \exp\left(-\frac{v_{xy}^2 \tau^2}{4m} \right)$$

$$g = \left(\frac{2\pi}{\lambda} \sigma_h (\cos\theta_i + \cos\theta_r) \right)^2$$

Q is a geometrical factor, D is a distribution function for the directional diffuse reflection term and g is the effective surface roughness. $\hat{k}_i$ and $\hat{k}_r$ are unit wave vectors in the incident and reflection directions, $\hat{s}_i, \hat{p}_i, \hat{s}_r$ and $\hat{p}_r$ are s and p polarization unit vectors of incident and reflection light. $\vec{v}$ is wave vector change and λ is wavelength of incident light.

For *S*, which takes into account the effect caused by shadowing and masking, we adopt the form introduced by Smith[11],

$$S(\theta_i,\theta_r,\sigma_h,\tau) = S_i(\theta_i)\cdot S(\theta_r) \tag{10}$$

where

$$S_i(\theta_i) = (1-\frac{1}{2}erfc(\frac{\tau\cot\theta_i}{2\sigma_h}))/(\Lambda(\cot\theta_i)+1)$$

$$S_r(\theta_r) = (1-\frac{1}{2}erfc(\frac{\tau\cot\theta_r}{2\sigma_h}))/(\Lambda(\cot\theta_r)+1)$$

$$\Lambda(\cot\theta) = \frac{1}{2}\left(\frac{2}{\sqrt{\pi}}\cdot\frac{\sigma_h}{\tau\cot\theta}-erfc(\frac{\tau\cot\theta}{2\sigma_h})\right)$$

$S_i(\theta_i)$ and $S_r(\theta_r)$ are shadowing and masking functions caused by incident and viewer direction respectively and *erfc* is the error function complement.

Substituting equations (9) and (10) into (8) and then into (7) we can find that the *BRDF* of the surface can be divided into two parts. We refer to the first item as the specular reflection, and the second part as directional diffuse reflection. On the other hand, we should know that the analysis above only take into account the first-surface reflection process, the uniform reflection due to multiple scattering and sub-surface reflection is not included. Therefore, we add one more item to the equation (7), and the total *BRDF* of the surface is:

$$f_r = f_{sp} + f_{dd} + f_{ud} \tag{11}$$

where

$$f_{sp} = \frac{|F|^2\cdot S\cdot e^{-g}\cdot\beta}{\cos\theta_i d\omega_r}\cdot\Delta \tag{12}$$

$$f_{dd} == \frac{|F|^2\cdot S\cdot d\omega_i\cdot\beta}{\pi\cos\theta_i\cos\theta_r d\omega_r}\cdot e^{-g}\cdot Q\cdot D \tag{13}$$

$$f_{ud} = \frac{\rho_0}{\pi} \tag{14}$$

f_{sp} represents the specular reflectivity of the surface, f_{dd} is the directional diffuse reflectivity and f_{ud} the uniform diffuse reflectivity of the surface. ρ_0 is diffuse reflection efficient, representing the fraction of incident energy that is reflected by the surface in uniform diffuse form.

The normalization constant β can be obtained by

$$\beta = \zeta\cdot\left(\iint G\cdot S d\theta_r d\phi_r\right)^{-1} \tag{15}$$

where ζ is a coefficient used to keep balance between diffuse reflection and once surface reflection. In our study, it was set at $1-\rho_0$.

For most materials used in woven clothes, surface of fibers may be relatively rough and *g*>>1 in equation (11). In rough surfaces, the specular reflection can be small and negligible. Then the reflection model for material surface can be simplified as follows and will be adopted in the derivations in next sections.

$$f_r \cong \frac{|F|^2\cdot S\cdot\beta\cdot Q\cdot d\omega_i\cdot\tau^2}{16\pi\cos\theta_i\cos\theta_r d\omega_r\sigma_h^2}\cdot\exp\left(-\frac{v_{xy}^2\tau^2}{4v_z^2\sigma_h^2}\right)+\frac{\rho_0}{\pi} \tag{16}$$

The followings show some properties of our proposed reflection model. Figure 3 is the reflectance of a slightly rough surface with σ_h/τ=0.05 for three different incident angles. The curves show the relative intensity of reflection light in the incident plane for a planar surface as a function of view angles. From left

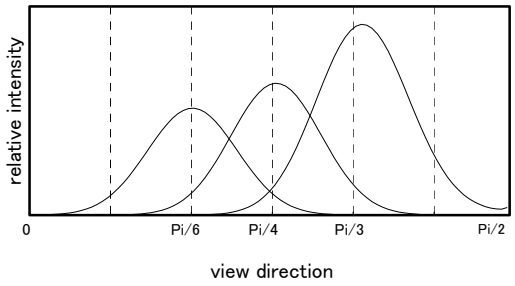

Figure 3: Reflection as function of view direction for different incident angle

to right the curves are for incident angle as π/6, π/4, π/3. The reflectance intensity will increase as the incident angle increases. This is caused by Fresnel reflection as well as geometrical factor. Reflectance intensity plots as function of surface roughness are showed in Figure 4. The incident angle is π/4. From the left to right the surface roughness σ_h/τ are 0.5, 0.4, 0.3, 0.2, 0.15, 0.1 and 0.05. All curves are in the incident plane. As surface roughness increases, reflectance near the incident

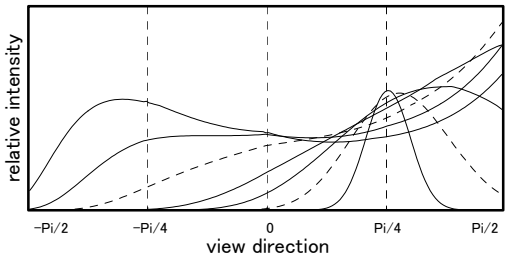

Figure 4: Reflection as function of view direction for different surface roughness

light also increases, this can explain that for rough surface, the surface will appear brighter as the direction of observation approaches the illumination direction. Figure 5 shows reflectance intensity as function of azimuth. From left to right the curves are for observation azimuth of π, 15π/16 and 11π/12. Surface roughness is 0.05. Reflectance will decrease as azimuth angle increases.

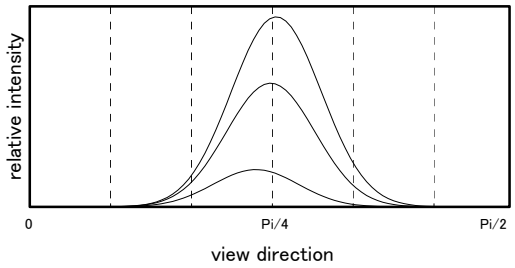

Figure 5: Reflection as function of view direction for different view azimuth

3. Reflection of Yarns

Yarns are usually consisted of many different kinds of fibers, parallel or twisted, tightly or loosen. Also there are many different shapes for the cross section of fibers. Yarns are usually simulated by small cylinders with infinite length in conventional models and it is reasonable to some extent. But it is also evident that the varieties of composed fibers will definitely result in more complex surface of yarns. More accurate model can be achieved from a group of parallel tightly bounded triangle prism with smooth arc corners. We will analyze the reflection from such structure caused by more complicated reflection model developed in Section 2.

3.1 Geometrical structure

The surface model and coordinate we used are showed in Figure 6. There are three parameters for the model, radius of arc, length of lateral and normals of lateral θ_a. The lateral is a tangent line of arc at the angle of normals. Because yarn is consisted of many fibers and the cross size of fibers is very small in comparison to their length, the intensity reflected off such a triangle prism can be approximated by the reflection of only one cross section of this structure.

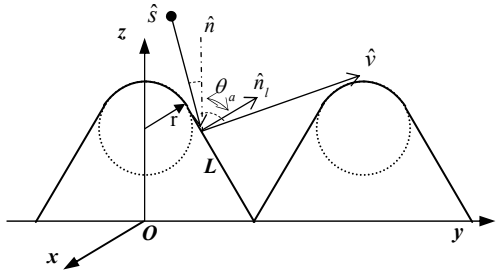

Figure 6: Surface model of yarns

Without lost generality, we take a unit radius for arc and *L* for the length of lateral which ranges from 0 to infinite. Moreover, the proposed surface model can be reduced to V-cavity model and Cylinder model at different conditions. When the normals of lateral θ_a equals to $\pi/2$, it will be Cylinder model and while the length of lateral *L* is approaching to infinite, it will be V-cavity model. It shows that not only the model can be applied to large scale surface, but also it can be used to simulation of more general rough surfaces.

3.2 Reflection derivation

When the incident and view angle are smaller than $\pi/2-\theta_a$, the surface is fully illuminated and completely visible. The projected radiance of the surface is

$$L_{rp}(\theta_i,\phi_i,\theta_r,\phi_r,\theta_a,\phi_a)=\frac{I_0}{2(L\cos\theta_a+\sin\theta_a)<\hat{v},\hat{n}>}\{A+B\} \tag{17}$$

where,

$$A=\sum_{n=1,2}\int_0^{\theta_a} f_{bd}<\hat{s},\hat{a}_n(\theta)><v,\hat{a}_n(\theta)>d\theta$$

$$B=\sum_{n=1,2} f_{bd}<\hat{s},\hat{a}_n(\theta_a)><\hat{v},\hat{a}_n(\theta_a)>\cdot L$$

ϕ_a is the orientation of fiber axis, I_0 is the irradiance of the incident light, $\hat{a}_n(\theta)$ is the normal of a point on the arc or the lateral, and *n* is the surface number of the two confronted surfaces.

When the incident light or viewer are from larger angles (larger than $\pi/2-\theta_a$), the surface is shadowed or masked by adjacent parts of it, and not all the surface can be illuminated or visible. The geometrical effects will affect the radiance received by the sensor and must be taken into account. This can be solved by geometrical attenuation factor that lies between 0 and 1 for the lateral parts. It is the reduction in the radiance of a lateral due to masking and shadowing effects and equals the ratio of the surface area that is both visible and illuminated to the total surface area. For arc parts, the actual angle ranges of the visible and illuminated can be solved by basic trigonometry. The total radiance can be corrected by replacing *A* and *B* in equation(18) by *A´* and *B´*:

$$A'=\sum_{n=1,2}\int_0^{\theta_n} f_{bd}<\hat{s},\hat{a}_n(\theta)><v,\hat{a}_n(\theta)>d\theta$$

$$B'=\sum_{n=1,2} f_{bd}<\hat{s},\hat{a}_n(\theta_a)><\hat{v},\hat{a}_n(\theta_a)>\eta_n L$$

The geometrical attenuation factor and key angles can be obtained using basic trigonometry as:

$$\eta_n=\left\{1,0,\frac{2\cos\theta_a\cos\theta_{mp}+\left[\sin(\theta_a+\theta_{mp})-1\right]/L}{\cos(\theta_a-\theta_{mp})}\right\}$$

$$\theta_n=\left\{\theta_a,\frac{\pi}{2}-\theta_{mp},\theta_{mp}+\arcsin\left[2(L\cos\theta_a+\sin\theta_a)\cos\theta_{mp}-1\right]\right\}$$

which values depend on the incident light and the viewer direction and the parameter θ_a. Footnote *n*=1,2

represents the confronted surface number, and *m*=*i*,*r* represents incident light and sensor, respectively. θ_{mp} is projections of incident light and sensor in the plane of fiber cross section.

The lateral surface considered above includes a fixed parameter θ_a, meaning the same slope of all laterals. Real surface can include a variety of different slope facets. Assume that the parameter has a distribution $P(\theta_a)$, the radiance of the surface can therefore be determined as:

$$L_r(\theta_i,\phi_i,\theta_r,\phi_r,\phi_a)=\int_0^{\frac{\pi}{2}} P(\theta_a)L_{rp}(\theta_i,\phi_i,\theta_r,\phi_r,\theta_a,\phi_a)d\theta_a \quad (18)$$

We assume the distribution of θ_a to be Gaussian-like, with μ mean and standard deviation σ, *i.e*:

$$P(\theta_a)=c\exp\left(-\frac{(\theta_a-\mu)^2}{2\sigma^2}\right)\cos\theta_a \quad (19)$$

where *c* is a normalization constant.

The interreflection between fibers is a little complicated. Interreflection between objects is often neglected in many reflectance models due to its complexities, and in fact its effect is considerably large in some cases and can not be ignored. Some analysis on interreflection had just taken such an assumption that the reflection of considered surface to be Lambertian or ideal specular. For reality, it is a more complicated reflection process and will make the calculation of interreflection more difficult. In our case, the radiance by interreflection, sub-radiance and multi-reflection has significant effect on the surface reflection, especially in the direction perpendicular to fibers axis. We will add a Lambertian item to explain these affects which depends on the incident and viewer azimuth angle. So the whole radiance will be:

$$L_r(\theta_i,\phi_i,\theta_r,\phi_r,\phi_a)=(1-\hbar)L_r(\theta_i,\theta_r,\phi_i,\phi_r,\phi_a)+\hbar I_0\rho\cos\theta_i \quad (20)$$

where $\hbar$ is a parameter which indicates the balance between model reflection and interreflection and has a value between 0 and 1.

Not all the yarns can be regarded as are consisted of regular parallel fibers and sometimes the fibers are twisted into threads. There is a profile for triangle prisms along axis direction, here we suggest it be a normal distribution $P(\phi_a)$, then the radiance will be:

$$L_r(\theta_i,\phi_i,\theta_r,\phi_r,0)=\int_{-\frac{\pi}{2}}^{\frac{\pi}{2}} P(\phi_a)L_r(\theta_i,\phi_i,\theta_r,\phi_r,\phi_a)d\phi_a \quad (21)$$

the distribution of $P(\phi_a)$ shows the extent of the fibers twisted.

On the other hand, for yarns with heavily loosen and twisted fibers, reflection from surface of yarns can be regarded as isotropic, i.e. the triangle prisms are uniformly distributed in all orientation in the plane of the surface. The result is a surface with isotropic roughness. Form the previous section, we have known the radiance of facets with single orientation ϕ_a, therefore, the radiance of the isotropic surface due to direct illumination is determined as an integral of the projected radiance over ϕ_a:

$$L_{rpp}(\theta_i,\phi_i,\theta_r,\phi_r)=\frac{1}{2\pi}\int_0^{2\pi} L_{rp}(\theta_i,\phi_i,\theta_r,\phi_r,\phi_a)d\phi_a \quad (22)$$

For different woven cloth, the visible weft and wrap yarns on the surface vary with different weaving structures. We introduce a distribution factor γ to describe the weight of the weft yarns, then the whole radiance is:

$$L_r(\theta_i,\phi_i,\theta_r,\phi_r)=\gamma L_r(\theta_i,\phi_i,\theta_r,\phi_r,0)+(1-\gamma)L_r(\theta_i,\phi_i,\theta_r,\phi_r,\frac{\pi}{2}) \quad (23)$$

4. Comparison with Experiments

In this section the reflectance model calculations is compared with actual measurement results. The reflection of the sample cloth was measured from multi points by holographic spectrophotometer with wavelength of 380*nm*~780*nm* and resolution of 2*nm*. The light source is a 500W halogen lamp. The sample cloth was placed on a rotary stage. Light source and spectrophotometer were fixed to be perpendicular to each other, both focusing on the sample cloth. The

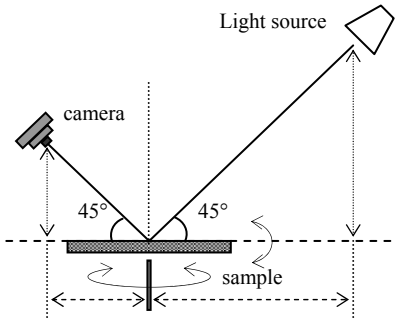

Figure 7: The measurement setup

stage can be rotated in the horizon plane at 45° step, and 3° step in the vertical plane (Figure 7)[10]. The reflectivity of the cloth was measured and the radiance was obtained by following equation:

$$L_e=\sum_{380}^{780}E(\lambda)\Delta\lambda \quad (24)$$

where L_r is the radiance of the sample cloth, $E(\lambda)$ is the spectrophotometer radiance for wavelength λ and $\Delta\lambda$ is wavelength resolution. In this experiment, $\Delta\lambda$ was 2*nm*. L_r has the unit of $W/sr\cdot m^2$.

Several kinds of cloth were tested. Figure 8 shows the results obtained for polyester sateen cloth sample and theoretical simulation results from our model. The polyester fibers have smooth surface, high reflectivity and the same triangle cross sections as silks, and are usually used to replace silk to obtain the same visual

effects. On the surface of such cloth, the weft yarns are almost invisible. The equation (20) is applied to describe its reflection. In the figure, ■, ▲ and × are the detected radiances for the source at the direction of weft, wrap and 45° from weft, respectively. The solid

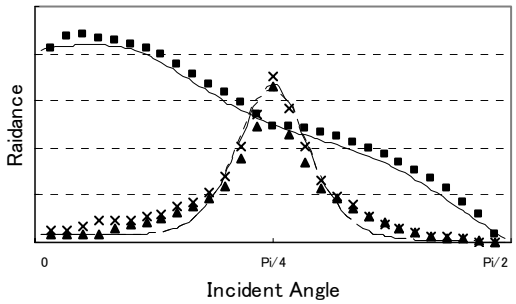

Figure 8: Simulation result for polyester sateen sample

line, dashed line and dotted lines are the estimations by our models for direction of the weft, wrap and from 45° from weft, respectively, with ϕ_a, σ_h/τ, L, μ and σ being set at 0, 0.05, 20, 0 and 1.2, respectively. From the results, we can know that the effect of masking and shadowing is high in the weft direction, while negligible in the wrap direction.

Similar results are presented in Figure 9 for belt cloth sample and Figure 10 for silk sample. In the two simulations, the structure of cloth can not be clearly

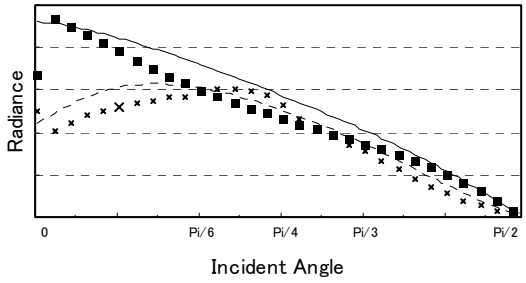

Figure 9: Simulation result for belt cloth sample

described with a clear geometrical top structure. For belt cloth sample, we use equation (21) and choose appropriate parameters to get satisfied simulation results. In Figure 9, ■ and × are the measured results observed from the weft direction and the wrap direction, respectively. The solid line and the dashed line are the calculation results with our model for the weft and wrap direction respectively. The results for the direction of 45° from the weft are the same with that of the wrap direction. In the case, the surface roughness of fibers for belt cloth sample was set at 0.2, meaning a relatively rough surface. In Figure 10, ■, ▲ and × are the measured radiances for the direction of weft, wrap and 45° from weft, respectively. we found that the reflections from the weft, wrap and 45° from the weft have almost the same characteristic, hinting an isotropic reflection, so we applied equation (22) to describe reflection for sample silk cloth. By manually choosing the appropriate surface roughness and standard deviation of Gaussian distribution, we found the results from our model agreeing with the actual results for both samples.

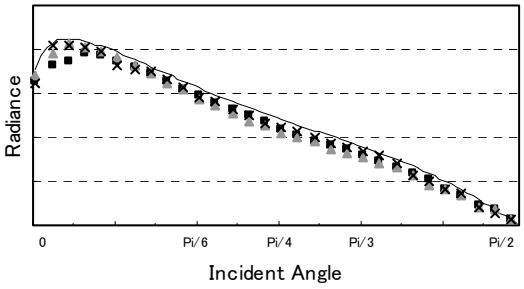

Figure 10: Simulation result for silk sample

5. Conclusion and Future Work

In this paper, we presented a physically-based reflectance model for the elements of woven clothes, fibers and threads, and proposed a framework to accomplish reflection simulation of woven cloth. The model agreed with experimental data taken from spectrophotometer measurements on samples of different woven textile and materials. The results show that the model is analytical and is applicable to all kinds of woven textile structures and different fiber matearials. It is also suitable for computer graphics application.

Future work includes determining relations between parameters and woven textile structure to make the model more applicable and operational.

References

[1] M. Oren and S. K. Nayar, Generalization of Lambert's reflectance model. *Proceedings of SIGGRAPH '94*, 1994, 239-246.

[2] K. E. Torrance, E. M. Sparrow, Theory for off-specular reflection from roughened surfaces. *Journal of the Optical Society of America*, 57, 1967, 1105-1114.

[3] R. L. Cook and K. E. Torrance, A Reflectance Model for Computer Graphics, *ACM Transactions on Graphics*, 1(1), 1981, 7-24.

[4] P. Poulin and A. Fournier, A model for anisotropic reflection. *ACM Computer Graphics* (*SIGGRAPH 90*), 24(4), 1990, 273-282.

[5] X. D. He, K. E. Torrance, F. X. Sillion, and D. P. Greenberg, A comprehensive physical model for light reflection, *ACM Computer Graphics* (*SIGGRAPH 91*), 25(4), 1991, 175-186.

[6] S. K. Nayar, K. Ikeuchi and T. Kanade, Surface reflection: physical and geometrical perspectives,

IEEE Transactions on Pattern Analysis and Machine Intelligence, 13(7), 1991, 611-634.
[7] Evelyn Chun-Yi Wang, Woven cloth simulation, http://userpages.umbc.edu/~cwang3/English/Spring00/CMSC635/project/finalpaper.html.
[8] C. Schlick, An inexpensive BRDF model for physically-based rendering, Proceeding of the International Conference Eurograhics '94, 13(3), 1994, 233-234.
[9] Vladimir V. Volevich, Andrei B. Khodulev, E. Kopylov, Olga A. Karpenko, An approach to cloth synthesis and visualization. The 7th International Conference on Computer Graphics and Visualization, Moscow, Russia, May, 1997.
[10] Usami, Creating anisotropic reflectance model of cloth based on analyzing reflection light, Master's thesis, Ritsumekan Univ., Japan, 1999.
[11] Smith, Bruce G, "Geometrical Shadowing of a Random Rough Surface", *IEEE Transactions on Antennas and Propagation*, AP-15(5), September 1967, 668-671.